DISCRETE TRAVELLING SOLITONS IN THE SALERNO MODEL

THOMAS R.O. MELVIN†, ALAN R. CHAMPNEYS† AND DMITRY E. PELINOVSKY††
† DEPARTMENT OF ENGINEERING MATHEMATICS, UNIVERSITY OF BRISTOL, BRISTOL BS8 1TR, UNITED KINGDOM
†† DEPARTMENT OF MATHEMATICS, MCMASTER UNIVERSITY, HAMILTON, ONTARIO, CANADA, L8S 4K1

Abstract. We investigate travelling solitary waves in the 1D Salerno model, which interpolates between the cubic discrete nonlinear Schrödinger (DNLS) equation and the integrable Ablowitz-Ladik (AL) model. In a travelling frame the model becomes an advance delay equation to which we analyse existence of homoclinic orbits to the rest state. The method of beyond all orders asymptotics is used to compute the so-called Stokes constant that measures the splitting of the stable and unstable manifolds. Through computing zeros of the Stokes constant, we find that there exists a number of solution families for parameter values between the DNLS and AL limits of the Salerno model. Using a pseudo-spectral method, we numerically continue these solution families and show that their parameters approach the curves of the zero level of the Stokes constant as the soliton amplitude approaches zero. An interesting topological structure of solutions occurs in parameter space. As the AL limit is approached solutions sheets of single-hump solutions undergo folds and become double-hump solitons. Numerical simulation suggest the single-humps to be stable and to interact almost inelastically.

1. Introduction. The existence of localised travelling waves in discrete nonlinear Schrödinger (DNLS) lattices has recently received a lot of attention (see e.g [7]). This is largely due to the experimental realisation of solitons in discrete media, such as waveguide arrays [3] and optically induced photorefractive crystals [8]. The prototypical equation that emerges from these models is the DNLS equation with some nonlinear term f, of the form

$$i\dot{u}_n(t) = \frac{u_{n+1}(t) - 2u_n(t) + u_{n-1}(t)}{h^2} + f(u_{n+1}(t), u_n(t), u_{n-1}(t)). \tag{1.1}$$

Finding travelling solitons which move without shedding any radiation, that is homoclinic orbits to the rest state in a moving frame, is a very delicate problem. Analysing travelling solutions with small wavespeed that bifurcate from the stationary solutions is problematic, as moving into the travelling frame introduces a large number of resonances in the spectrum of the linear operator which give rise to radiation modes. To minimise the number of these radiation modes it is necessary to look for solutions that travel with a *finite* wavespeed [12], that is in an appropriate region of parameter space where the minimum wavespeed is bounded away from zero. However, posing the DNLS in a travelling frame gives rise to a differential advance-delay equation which is notoriously hard to analyse. Recent progress in this area has been made by developing a Melnikov method around existing solution families [16] or by using a pseudo-spectral method to transform the advance-delay equation into a large system of algebraic equations [2, 13]. Alternatively, looking for small-amplitude (but non-zero wavespeed) solutions bifurcating from the rest state involves computation of the so-called Stokes constants [20] in the method of beyond all orders asymptotics which measure the splitting of the stable and unstable manifolds. This problem was considered in [14] for the DNLS with a saturable nonlinear term, where a number of zeros of the Stokes constant were found for a sufficiently large saturation parameter. This paper concerns derivation and computation of the Stokes constant for the Salerno model [19] with the nonlinear function

$$f = 2(1-\alpha)\left|u_n\right|^2 u_n + \alpha\left|u_n\right|^2 (u_{n+1} + u_{n-1}). \tag{1.2}$$

The Salerno model is a DNLS equation which interpolates between the cubic DNLS model [11] at $\alpha = 0$ and the integrable Ablowitz-Ladik (AL) model [1] at $\alpha = 1$. The Salerno model was also derived from the Gross-Pitaevskii equation for Bose-Einstein condensates with magnetic momentum [10]. It is well known [17] that no single-humped localised travelling waves exist in the DNLS with pure cubic nonlinearity, $\alpha = 0$, because single-humped solitons are surrounded by non-decaying oscillatory tails. However, models with an exceptional discretisation of the cubic term in the DNLS equation often support localised travelling waves. These include the AL lattice [9] and the translationally invariant lattice derived in [15]. The Salerno model has a two-parameter family of exact travelling solitary wave solutions at $\alpha = 1$ corresponding to the AL lattice, however, these solutions do not persist for $\alpha \neq 1$ away from the integrable limit [9]; this result has been confirmed using a Melnikov method in [16]. However, further numerical results in [16] suggest that the Salerno model can still support travelling solutions for some $\alpha \neq 1$ far from the integrable limit. The existence of travelling waves in the Salerno model for $\alpha \in (0, 1)$ is the subject of this paper.

The paper is set out as follows. In Section 2 we derive a regular asymptotic solution to the Salerno model. Although this solution is correct to all orders of the asymptotic expansion, it does not capture the radiation tails as these terms are exponentially small in the bifurcation parameter and hence lie beyond all orders of the expansion. In Section 3 we use the method of beyond-all-order asymptotics (see [14], [20] and references therein) to analytically continue

the expansion into the complex plane where the asymptotic expansion blows up. The Stokes constants measure the residue coefficients of the singular part of the beyond-all-order terms corresponding to the splitting between stable and unstable manifolds. Section 4 deals with computation of the Stokes constant in the region of parameter space where there is only one radiation mode. We find that for suitable parameter values there exist a number of zeros corresponding to travelling wave solutions to the Salerno model. Using a pseudo-spectral method [6, 5] in Section 5, we compute the travelling solitons and show that their parameters approach the curves for the zero level of the Stokes constant as the soliton amplitude is reduced. Finally, we sum up our conclusions and discuss open problems in Section 6.

2. Regular Asymptotic Expansion. Taking equation (1.1) we look for travelling solutions of the form

$$u_n(t) = \phi(hn + 2ct)e^{-i\omega t}, \qquad \phi : \mathbb{R} \mapsto \mathbb{C}, \quad \omega, c \in \mathbb{R}$$

where ω is the temporal frequency and c is the wavespeed of the travelling solutions. Moving into the travelling frame $z = hn + 2ct \in \mathbb{R}$ gives the differential advance-delay equation,

$$2ic\phi'(z) = \frac{\phi(z+h) - 2\phi(z) + \phi(z-h)}{h^2} - \omega\phi(z) + f(\phi(z+h), \phi(z), \phi(z-h)), \tag{2.1}$$

where f is given by (1.2) for the Salerno model. We are interested in localised solutions to (2.1), i.e. modes for which $\phi(z) \to 0$ as $z \to \pm\infty$. It is convenient to use the transformation of variables,

$$\phi(z) = \frac{\kappa}{h}\Phi(Z)e^{i\beta Z/\kappa}, \quad z = \frac{hZ}{\kappa}, \tag{2.2}$$

and the parameterization

$$\omega = \frac{2}{h}\beta c + \frac{2}{h^2}\left[\cos(\beta)\cosh(\kappa) - 1\right], \quad c = \frac{1}{h\kappa}\sin(\beta)\sinh(\kappa), \tag{2.3}$$

where $\kappa \in \mathbb{R}_+$ and $\beta \in [0, 2\pi]$. Substitution of (2.2)–(2.3) into (2.1) gives an equation for $\Phi(Z)$ in the form

$$\begin{aligned}&\cos(\beta)\left[\Phi(Z+\kappa) + \Phi(Z-\kappa) - 2\cosh(\kappa)\Phi(Z)\right] + i\sin(\beta)\left[\Phi(Z+\kappa) - \Phi(Z-\kappa) - 2\sinh(\kappa)\Phi'(Z)\right]\\ &+\kappa^2 f\left(\Phi(Z+\kappa)e^{i\beta}, \Phi(Z), \Phi(Z-\kappa)e^{-i\beta}\right) = 0,\end{aligned} \tag{2.4}$$

where we have used that f is a homogeneous cubic polynomial. Bifurcations of traveling wave solutions may occur in the limit $\kappa \to 0$ [17]. The curve $\kappa = 0$ gives a boundary of the existence domain on the (ω, c)-plane shown in Figure 2.1.

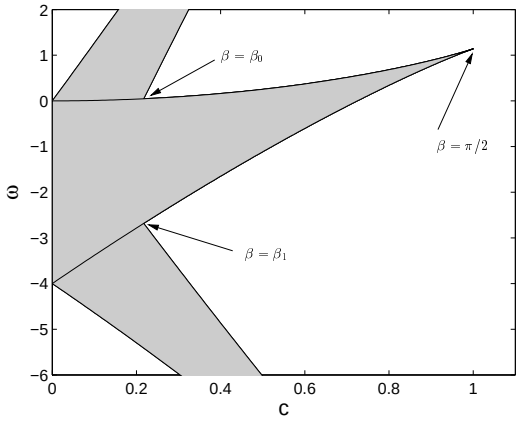

FIG. 2.1. *Bifurcation curve $\kappa = 0$ on the (ω, c)-plane for $h = 1$. Localized solutions of the differential advance-delay equation (2.4) may bifurcate from the boundary to the white region (with $\kappa \in \mathbb{R}_+$). For $\beta < \beta_0$ and $\beta > \beta_1$, more than one radiation mode exists.*

We call the equation in the form (2.4) as the outer equation for the bifurcation. We now seek to form a regular asymptotic expansion of the outer equation in powers of κ. The advance and delay terms are expanded as a Taylor

series,

$$\Phi(Z+\kappa)+\Phi(Z-\kappa)-2\cosh(\kappa)\Phi(Z)=\kappa^2[\Phi''(Z)-\Phi(Z)]+\frac{\kappa^4}{12}[\Phi''''(Z)-\Phi(Z)]+O(\kappa^6),$$
$$\Phi(Z+\kappa)-\Phi(Z-\kappa)-2\sinh(\kappa)\Phi'(Z)=\frac{\kappa^3}{3}[\Phi'''(Z)-\Phi'(Z)]+O(\kappa^5),$$

while the nonlinear function f is expanded as

$$\begin{aligned} f =& 2[1+\alpha(\cos(\beta)-1)]\left|\Phi(Z)\right|^2\Phi(Z)+2i\kappa\alpha\sin(\beta)\left|\Phi(Z)\right|^2\Phi'(Z)\\ &+\kappa^2\alpha\cos(\beta)\left|\Phi(Z)\right|^2\Phi''(Z)+O(\kappa^3). \end{aligned}$$

We seek an outer asymptotic expansion for $\Phi(Z)$ of the form $\Phi(Z)=\sum_{n=0}^{\infty}(i\kappa)^n\Phi_n(Z)$. Substituting this expansion into (2.4) gives to leading order, $O(\kappa^2)$,

$$\cos(\beta)[\Phi_0''(Z)-\Phi_0(Z)]+2[1+\alpha(\cos(\beta)-1)]\left|\Phi_0(Z)\right|^2\Phi_0(Z)=0,$$

which has a real-valued solution

$$\Phi_0(Z)=S\,\mathrm{sech}\,(Z),\quad S=\frac{\sqrt{\cos(\beta)}}{\sqrt{1+\alpha(\cos(\beta)-1)}} \tag{2.5}$$

if $S\in\mathbb{R}$. The region of parameter space for which this holds, bounded by the curves $\beta=\frac{\pi}{2}$, $\beta=\beta^*(\alpha)$, and $\beta=\pi$, is shown in Figure 2.2.

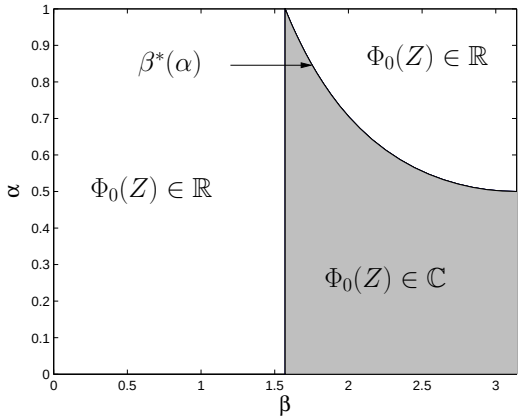

FIG. 2.2. *Parameter regions, for which solution (2.5) is real-valued (white) and complex-valued (shaded).*

At the next order, $O(\kappa^3)$, we obtain a linear inhomogeneous equation for a real-valued $\Phi_1(Z)$ in the form

$$L_-\Phi_1=\frac{2\sin(\beta)S^3(1-\alpha)}{\cos^2(\beta)}\mathrm{sech}^3(Z)\tanh(Z), \tag{2.6}$$

where $L_-=-\partial_Z^2+1-2\mathrm{sech}^2(Z)$. Since $L_-\Phi_0=0$ and $\Phi_0(Z)$ is an even function on $\mathbb{R}$, while the right-hand-side of (2.6) is an odd function on $\mathbb{R}$, a unique odd solution exists for $\Phi_1(Z)$, in fact in the explicit form $\Phi_1(Z)=\frac{\sin(\beta)S^3(1-\alpha)}{2\cos^2(\beta)}\mathrm{sech}(Z)\tanh(Z)$. Note that this term is zero for the AL lattice ($\alpha=1$), as an exact solution of the differential advance-delay equation (2.4) with $\alpha=1$ exists in the form $\Phi=\Phi_0(Z)=\mathrm{sech}(Z)$.

To compute the solution to higher orders, $O(\kappa^n)$ for $n\geq 4$, we have to solve a system of inhomogeneous linear equations separately in odd and even orders of n:

$$L_+\Phi_{2k}=g_{2k}(\Phi_0,\Phi_1,...,\Phi_{2k-1}),\quad L_-\Phi_{2k+1}=g_{2k+1}(\Phi_0,\Phi_1,...,\Phi_{2k}),\quad k\in\mathbb{N}, \tag{2.7}$$

where $L_+=-\partial_Z^2+1-6\mathrm{sech}^2(Z)$ and $g_n(\Phi_0,\Phi_1,...,\Phi_{n-1})$ is a polynomial function of the lower order terms. It is easy to check that $g_{2k}(Z)$ is even on $\mathbb{R}$, while $g_{2k+1}(Z)$ is odd on $\mathbb{R}$. Since $L_+\Phi_0'=0$ and $L_-\Phi=0$, where

$\Phi'(Z)$ is odd on $\mathbb{R}$ and $\Phi_0(Z)$ is even on $\mathbb{R}$, respectively, there exists a unique solution of the linear inhomogeneous equations (2.7) in the space of even functions for $\Phi_{2k}(Z)$ and odd functions for $\Phi_{2k+1}(Z)$. Therefore, the asymptotic expansion for $\Phi(Z)$ can be computed up to any order of κ. However, this expansion does not capture the behavior of the oscillatory tail as its amplitude is exponentially small as $\kappa \to 0$ and hence the oscillatory tail lies beyond all orders of the asymptotic expansion.

3. Beyond All Orders Asymptotic Expansion. The radiation tail to a traveling wave solution may appear in the solution to the outer equation (2.4) only beyond all orders of the asymptotic expansion in powers of κ. By analysing the outer expansion near to a singularity in the complex Z plane and by rescaling dependent and independent variables with the blow-up technique [20], the amplitude of the radiation tail can be measured at the leading-order approximation. The leading order term of the outer expansion, $\Phi_0(Z) = S\text{sech}\,(Z)$, has its first singularity at $Z = \frac{i\pi}{2}$. Therefore, we take

$$\psi(\zeta) = \kappa\Phi(Z), \quad \theta(\zeta) = \kappa\overline{\Phi}(Z), \quad Z = \kappa\zeta + \frac{i\pi}{2}, \tag{3.1}$$

where $\zeta \in \mathbb{C}$ and $\overline{\theta} \neq \psi$. The change of coordinates leads to a system of equations, which is called inner equations for bifurcation of traveling wave solutions,

$$\begin{aligned}
&\cos(\beta)\left[\psi(\zeta+1) + \psi(\zeta-1) - 2\cosh(\kappa)\psi(\zeta)\right] \\
&+ i\sin(\beta)\left[\psi(\zeta+1) - \psi(\zeta-1) - \frac{2\sinh(\kappa)}{\kappa}\psi'(\zeta)\right] + F(\psi,\theta) = 0, \\
&\cos(\beta)\left[\theta(\zeta+1) + \theta(\zeta-1) - 2\cosh(\kappa)\theta(\zeta)\right] \\
&- i\sin(\beta)\left[\theta(\zeta+1) - \theta(\zeta-1) - \frac{2\sinh(\kappa)}{\kappa}\theta'(\zeta)\right] + G(\psi,\theta) = 0,
\end{aligned} \tag{3.2}$$

where

$$\begin{aligned}
F &= 2(1-\alpha)\psi^2(\zeta)\theta(\zeta) + \alpha\psi(\zeta)\theta(\zeta)\left(\cos(\beta)[\psi(\zeta+1) + \psi(\zeta-1)] + i\sin(\beta)[\psi(\zeta+1) - \psi(\zeta-1)]\right), \\
G &= 2(1-\alpha)\psi(\zeta)\theta^2(\zeta) + \alpha\psi(\zeta)\theta(\zeta)\left(\cos(\beta)[\theta(\zeta+1) + \theta(\zeta-1)] - i\sin(\beta)[\theta(\zeta+1) - \theta(\zeta-1)]\right).
\end{aligned}$$

Solutions to the system of inner equations are expanded in powers of κ as

$$\psi(\zeta) = \psi_0(\zeta) + \sum_{n=1}^{\infty}\kappa^{2n}\psi_n(\zeta), \quad \theta(\zeta) = \theta_0(\zeta) + \sum_{n=1}^{\infty}\kappa^{2n}\theta_n(\zeta). \tag{3.3}$$

Substituting (3.3) into (3.2) gives to leading order, $O(\kappa^0)$,

$$\begin{aligned}
&\cos(\beta)\left[\psi_0(\zeta+1) + \psi_0(\zeta-1) - 2\psi_0(\zeta)\right] + i\sin(\beta)\left[\psi_0(\zeta+1) - \psi_0(\zeta-1) - 2\psi_0'(\zeta)\right] + F(\psi_0,\theta_0) = 0, \\
&\cos(\beta)\left[\theta_0(\zeta+1) + \theta_0(\zeta-1) - 2\theta_0(\zeta)\right] - i\sin(\beta)\left[\theta_0(\zeta+1) - \theta_0(\zeta-1) - 2\theta_0'(\zeta)\right] + G(\psi_0,\theta_0) = 0.
\end{aligned}$$

Note that we are interested in the limit $\kappa \to 0$ and therefore we will need to solve these equations to the leading order only [20]. By continuing the inner asymptotic expansion, we shall use the inverse power series for $\psi_0(\zeta) = \sum_{n=1}^{\infty}\frac{a_n}{\zeta^n}$ and $\theta_0(\zeta) = \sum_{n=1}^{\infty}\frac{b_n}{\zeta^n}$. Substituting these inverse power series into the system of equations gives at leading order, $O(\zeta^{-3})$,

$$a_1S^2 + a_1^2b_1 = 0, \quad b_1S^2 + b_1^2a_1 = 0, \tag{3.4}$$

which has a symmetric solution $a_1 = b_1 = -iS$. This solution corresponds to the leading-order term in the expansion of $\Phi_0(Z) = S\text{sech}(Z)$ with $Z = \kappa\zeta + \frac{i\pi}{2}$ as $\kappa \to 0$. We shall now consider the convergence of the inverse power series for $\psi_0(\zeta)$ and $\theta_0(\zeta)$. First, by substituting $\theta_0(\zeta) = e^{-p\zeta}$ into the second equation of the leading-order system of inner equations with $G \equiv 0$, we define the dispersion relation in the form

$$D(p;\beta) \equiv \cos(\beta)[\cosh(p) - 1] + i\sin(\beta)[\sinh(p) - p] = 0. \tag{3.5}$$

By substituting $\psi_0(\zeta) = e^{-p\zeta}$ into the first equation of the system with $F \equiv 0$, we obtain the dispersion relation in the form $\bar{D}(p;\beta) = 0$. Examining roots of $D(p;\beta)$, we can see that $p = 0$ is a triple root if $\beta = \frac{\pi}{2}$ and a double root if $\beta \neq \frac{\pi}{2}$. If $\beta = \frac{\pi}{2}$, there are no other purely imaginary roots of D. Analysis near this special point was reported in [17], in this situation the radiation modes do not appear as beyond all orders terms but instead only a third-order differential equation needs to be solved. We are interested in the existence of solutions away from this special point, when the radiation modes are beyond all orders. If $\beta \neq \frac{\pi}{2}$, then $p = 0$ is a double root of $D(p;\beta)$ and there also exists a varying number of imaginary roots, $p \in i\mathbb{R}$, depending upon the value of β. If $\beta \in (0,\pi)$ (that is $c > 0$), there are finitely many roots $p \in i\mathbb{R}$ for any value of β. Let $p = ik_0$ be the smallest root of $D(p;\beta)$ on the imaginary axis, moreover k_0 is the only non-zero root on the imaginary axis for $\beta \in (\beta_0, \beta_1)$, where $\beta_0 \approx \frac{\pi}{13}$ and $\beta_1 \approx \frac{13\pi}{14}$, see Figure 2.1. A symmetric root $p = -ik_0$ exists for $\bar{D}(p;\beta)$. Owing to the resonance caused by the roots $p = \pm ik_0$, the solution to the system of inner equations could have an oscillatory tail as $|\operatorname{Re}(\zeta)| \to \infty$, therefore we now consider a linearisation around the inverse power series for $\psi_0(\zeta)$ and $\theta_0(\zeta)$. To accommodate both cases $k_0 > 0$ and $k_0 < 0$, we write

$$\psi_0(\zeta) = \frac{-iS}{\zeta} + \Gamma\hat{\psi}(\zeta)e^{-i|k_0|\zeta} + \sum_{n=2}^{\infty}\frac{a_n}{\zeta^n}, \quad \theta_0(\zeta) = \frac{-iS}{\zeta} + \Gamma\hat{\theta}(\zeta)e^{-i|k_0|\zeta} + \sum_{n=2}^{\infty}\frac{b_n}{\zeta^n}, \tag{3.6}$$

where the exponential term $e^{-i|k_0|\zeta} = e^{-\frac{\pi|k_0|}{2\kappa}}e^{-\frac{ik_0 Z}{\kappa}}$ describes the beyond all orders effects as the term $e^{-\frac{\pi|k_0|}{2\kappa}}$ is exponentially small as $\kappa \to 0^+$. The coefficient Γ is a measure of the amplitude of the oscillatory tail so that a localised solution exists only if $\Gamma = 0$. Substituting (3.6) into the system of inner equations at the leading order and truncating the nonlinear terms to $O(\zeta^{-3})$ gives a linearized system for $\hat{\psi}(\zeta)$ and $\hat{\theta}(\zeta)$ in the form

$$\begin{aligned}
&\cos(\beta)\left[\hat{\psi}(\zeta+1)e^{-i|k_0|} + \hat{\psi}(\zeta-1)e^{i|k_0|} - 2\hat{\psi}(\zeta)\right]\left(1 - \frac{\alpha S^2}{\zeta^2}\right)\\
&+ i\sin(\beta)\left[\left(\hat{\psi}(\zeta+1)e^{-i|k_0|} - \hat{\psi}(\zeta-1)e^{i|k_0|}\right)\left(1 - \frac{\alpha S^2}{\zeta^2}\right) - 2\hat{\psi}'(\zeta) + 2i|k_0|\hat{\psi}(\zeta)\right]\\
&- \frac{2\cos(\beta)}{\zeta^2}\left(2\hat{\psi}(\zeta) + \hat{\theta}(\zeta)\right) + \mathrm{O}(\zeta^{-3}) = 0,\\
&\cos(\beta)\left[\hat{\theta}(\zeta+1)e^{-i|k_0|} + \hat{\theta}(\zeta-1)e^{i|k_0|} - 2\hat{\theta}(\zeta)\right]\left(1 - \frac{\alpha S^2}{\zeta^2}\right)\\
&- i\sin(\beta)\left[\left(\hat{\theta}(\zeta+1)e^{-i|k_0|} - \hat{\theta}(\zeta-1)e^{i|k_0|}\right)\left(1 - \frac{\alpha S^2}{\zeta^2}\right) - 2\hat{\theta}'(\zeta) + 2i|k_0|\hat{\theta}(\zeta)\right]\\
&- \frac{2\cos(\beta)}{\zeta^2}\left(2\hat{\theta}(\zeta) + \hat{\psi}(\zeta)\right) + \mathrm{O}(\zeta^{-3}) = 0.
\end{aligned} \tag{3.7}$$

Using a Laurent expansion for $\hat{\psi}(\zeta)$ and $\hat{\theta}(\zeta)$ with some integer exponent r, yet to be determined,

$$\begin{aligned}
\hat{\psi}(\zeta) =& \rho_1\zeta^r + \rho_2\zeta^{r-1} + \rho_3\zeta^{r-2} + O(\zeta^{r-3}),\\
\hat{\theta}(\zeta) =& \eta_1\zeta^r + \eta_2\zeta^{r-1} + \eta_3\zeta^{r-2} + O(\zeta^{r-3}),
\end{aligned}$$

the linearized system (3.7) can be solved at each successive power of r, giving for the $\hat{\psi}(\zeta)$ equation:

$$\begin{aligned}
O(\zeta^r) \quad & \rho_1 D(-i|k_0|;\beta) = 0,\\
O(\zeta^{r-1}) \quad & \rho_2 D(-i|k_0|;\beta) + \rho_1 r D'(-i|k_0|;\beta) = 0,\\
O(\zeta^{r-2}) \quad & \rho_3 D(-i|k_0|;\beta) + \rho_2(r-1)D'(-i|k_0|;\beta) + \rho_1\frac{r(r-1)}{2}D''(-i|k_0|;\beta)\\
& - \cos(\beta)\,(2\rho_1 + \eta_1) - \sin(\beta)\alpha S^2|k_0|\rho_1 = 0,
\end{aligned}$$

and for the $\hat{\theta}(\zeta)$ equation:

$$\begin{aligned}
O(\zeta^r) \quad & \eta_1 D(i|k_0|;\beta) = 0, \\
O(\zeta^{r-1}) \quad & \eta_2 D(i|k_0|;\beta) + \eta_1 r D'(i|k_0|;\beta) = 0, \\
O(\zeta^{r-2}) \quad & \eta_3 D(i|k_0|;\beta) + \eta_2 (r-1) D'(i|k_0|;\beta) + \eta_1 \frac{r(r-1)}{2} D''(i|k_0|;\beta) \\
& - \cos(\beta)\,(2\eta_1 + \rho_1) + \sin(\beta)\alpha S^2 |k_0| \eta_1 = 0,
\end{aligned}$$

where derivatives of $D(p;\beta)$ are taken with respect to p at $p = \pm i|k_0|$. If $\beta < \frac{\pi}{2}$, then $k_0 > 0$ and $p = ik_0$ is a root of $D(p;\beta)$ but not a root of $\bar{D}(p;\beta)$. Therefore, $D(i|k_0|;\beta) = 0$ and $D(-i|k_0|;\beta) \neq 0$ for $\beta < \frac{\pi}{2}$. To avoid the trivial solution, we normalize $\eta_1 = 1$, choose $r = 0$, and obtain therefore unique values for the coefficients of the power series, e.g.

$$\rho_1 = 0, \quad \rho_2 = 0, \quad \rho_3 = \frac{\cos(\beta)}{D(-i|k_0|;\beta)}, ..., \quad \eta_1 = 1, \quad \eta_2 = \frac{-2\cos(\beta) + \sin(\beta)\alpha S^2 |k_0|}{D'(i|k_0|;\beta)}, ... \tag{3.8}$$

The solution so far is:

$$\begin{aligned}
\psi_0(\zeta) =& \frac{-iS}{\zeta} + \Gamma \left[\frac{\cos(\beta)}{D(-i|k_0|;\beta)} \frac{1}{\zeta^2} + O\left(\frac{1}{\zeta^3}\right) \right] e^{-i|k_0|\zeta} + \sum_{n=2}^{\infty} \frac{a_n}{\zeta^n}, \\
\theta_0(\zeta) =& \frac{-iS}{\zeta} + \Gamma \left[1 + \frac{-2\cos(\beta) + \sin(\beta)\alpha S^2 |k_0|}{D'(i|k_0|;\beta)} \frac{1}{\zeta} + O\left(\frac{1}{\zeta^2}\right) \right] e^{-i|k_0|\zeta} + \sum_{n=2}^{\infty} \frac{b_n}{\zeta^n}.
\end{aligned} \tag{3.9}$$

If $\beta > \frac{\pi}{2}$, then $k_0 < 0$, such that $D(-i|k_0|;\beta) = 0$ and $D(i|k_0|;\beta) \neq 0$. As a result, the role of components $\hat{\psi}(\zeta)$ and $\hat{\theta}(\zeta)$ is swapped, compared to the previous solution (3.8)–(3.9) for $\beta < \frac{\pi}{2}$. We will develop explicit formalism for the case $\beta < \frac{\pi}{2}$, leaving the other case for a reader's exercise.

The system of inner equations for $\psi_0(\zeta)$ and $\theta_0(\zeta)$ can be reformulated as a system of integral equations using the Borel-Laplace transform [20]:

$$\psi_0(\zeta) = \int_\gamma V(p) e^{-p\zeta} dp, \quad \theta_0(\zeta) = \int_\gamma W(p) e^{-p\zeta} dp, \tag{3.10}$$

which gives

$$\begin{aligned}
&\overline{D}(p;\beta) V + V * W * \left(\left[(1-\alpha) + \alpha\cos(\beta)\cosh(p) - i\alpha\sin(\beta)\sinh(p) \right] V \right) = 0, \\
&D(p;\beta) W + W * V * \left(\left[(1-\alpha) + \alpha\cos(\beta)\cosh(p) + i\alpha\sin(\beta)\sinh(p) \right] W \right) = 0.
\end{aligned} \tag{3.11}$$

Here the star represents the convolution operator defined by

$$(V * W)(p) = \int_0^p V(p - p_1) W(p_1) dp_1, \tag{3.12}$$

where the integration is performed along a curve from the origin to the point p in the complex plane. Now consider two solutions $\{\psi_0^s(\zeta), \theta_0^s(\zeta)\}$ and $\{\psi_0^u(\zeta), \theta_0^u(\zeta)\}$ which lie on the stable and unstable manifolds respectively such that

$$\begin{aligned}
\lim_{\mathrm{Re}(\zeta)\to+\infty} \psi_0^s(\zeta) &= \lim_{\mathrm{Re}(\zeta)\to+\infty} \theta_0^s(\zeta) = 0, \\
\lim_{\mathrm{Re}(\zeta)\to-\infty} \psi_0^u(\zeta) &= \lim_{\mathrm{Re}(\zeta)\to-\infty} \theta_0^u(\zeta) = 0.
\end{aligned} \tag{3.13}$$

If a homoclinic orbit exists, then these two solutions coincide. The Borel-Laplace transform (3.10) generates the solution on the stable manifold when the contour of integration γ_s lies in the first quadrant of the complex p-plane and produces the solution on the unstable manifold if it lies in the second quadrant. If there are no singularites between the two integration contours γ_s and γ_u, then the contours could be continuously deformed into each other implying that the

solution generated by each contour is the same, i.e. $\psi_0^s(\zeta) = \psi_0^u(\zeta)$ and $\theta_0^s(\zeta) = \theta_0^u(\zeta)$, therefore the amplitude of the oscillatory tail Γ would be zero and a localised travelling wave would exist. However, as mentioned previously, there is at least one resonance $p = i|k_0|$ on the positive imaginary axis (we ignore the singularities which have $\mathrm{Re}(p) \neq 0$ as it is always possible to define γ_s and γ_u to lie above these points) and so deformation of the integration contours lead to a residue contribution around the singularity at $p = i|k_0|$, see Figure 3. Apart from the double root at $p = 0$, $p = ik_0$ is the only root on the positive imaginary axis for $\beta_0 < \beta < \beta_1$ and all other roots are bounded away from $\mathrm{Re}(p) = 0$.

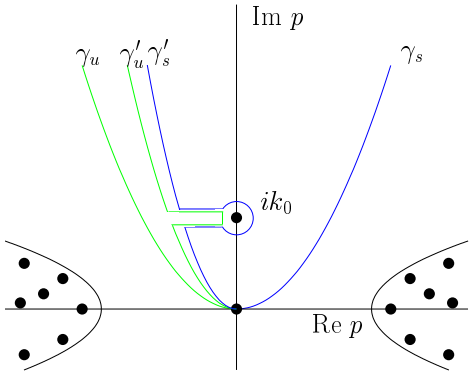

FIG. 3.1. *Integration contours, γ, around the root ik_0, where dots indicate roots of $D(p;\beta)$.*

Let us now put into correspondence the behaviour of the leading order terms $\psi_0(\zeta)$ and $\theta_0(\zeta)$ as given by (3.9) and the poles of $V(p)$ and $W(p)$. To generate the expansion (3.9), the functions $V(p)$ and $W(p)$ must be of the form

$$\begin{aligned} V(p) =& O\left((p - i|k_0|)\log(p - i|k_0|)\right) - iS + \sum_{n=2}^{\infty} a_n p^{n-1}, \\ W(p) =& \frac{\Gamma}{2\pi i(p - i|k_0|)} + O(\log(p - i|k_0|)) - iS + \sum_{n=2}^{\infty} b_n p^{n-1}, \end{aligned} \tag{3.14}$$

where the logarithmic terms arise from the terms $O(\zeta^{-m})e^{-i|k_0|\zeta}$ with $m \geq 1$. The constant Γ is referred to as the Stokes constant for $p = i|k_0|$. Only if the constant Γ is zero, may there exist a homoclinic orbit to the rest state, and therefore there may exist a localised travelling wave. All other singular terms in the expansion (3.14) are subordinate to the simple pole with the residue coefficient Γ. The inverse power series in ζ for $\psi_0(\zeta)$ and $\theta_0(\zeta)$ become the power series expansions in p for $V(p)$ and $W(p)$,

$$V(p) = \sum_{n=0}^{\infty} V_n p^n, \quad W(p) = \sum_{n=0}^{\infty} W_n p^n, \tag{3.15}$$

which converges in the neighborhood of the origin. The power series (3.15), however, diverges as $p \to i|k_0|$, where it should recover the pole singularity of the solution (3.14), according to the matching condition

$$\sum_{n=0}^{\infty} W_n p^n \xrightarrow[p \to i|k_0|]{} \frac{\Gamma}{2\pi|k_0|} \frac{1}{1 + \frac{ip}{|k_0|}} = \frac{\Gamma}{2\pi|k_0|} \sum_{n=0}^{\infty} \frac{(-ip)^n}{|k_0|^n}. \tag{3.16}$$

The Stokes constant is hence given by

$$\Gamma = 2\pi|k_0| \lim_{n \to \infty} (i|k_0|)^n W_n. \tag{3.17}$$

We shall use this formula for numerical computations of the Stokes constant.

4. Computation of the Stokes constant. We will now compute the Stokes constant by computing the limit (3.17). Since we consider power series solutions (3.15) of the system of integral equations (3.11), we expand the dispersion relation $D(p;\beta)$ as a power series

$$D(p;\beta) = \cos(\beta)\sum_{n=1}^{\infty}\frac{p^{2n}}{(2n)!} + i\sin(\beta)\sum_{n=1}^{\infty}\frac{p^{2n+1}}{(2n+1)!}. \tag{4.1}$$

The convolution operator for power series solutions (3.15) becomes

$$(V*W)(p) = \sum_{n_1=0}^{\infty}\sum_{n_2=0}^{\infty}\frac{n_1!n_2!}{(n_1+n_2+1)!}V_{n_1}W_{n_2}p^{n_1+n_2+1}. \tag{4.2}$$

Substituting (3.15), (4.1) and (4.2) into system (3.11) gives a power series in p that can be solved for each value of n to give coefficients (V_n, W_n) in terms of the preceding coefficients $\{(V_m, W_m),\ 0 \le m < n\}$. The first two terms of the power series (3.15) are

$$\begin{aligned} n = 2 &\to V_0 = W_0 = -iS, \\ n = 3 &\to V_1 = -W_1 = \frac{\sin(\beta)S^3(1-\alpha)}{2\cos^2(\beta)}. \end{aligned}$$

Obtaining a good approximation for coefficients V_n and W_n, when n is large, is computationally difficult owing to V_n and W_n becoming either very large or very small in the large n limit. To improve the performance of the numerical computations, it is advantageous to normalise the coefficients by using the limit (3.17). Since the symmetry of equations implies that $W(p) = V(-p)$, see [14], we use the substitution

$$V_n = \frac{-i(-1)^n\tau_n}{(i|k_0|)^n}, \quad W_n = \frac{-i\tau_n}{(i|k_0|)^n}, \quad n \in \mathbb{N}, \tag{4.3}$$

with $\tau_0 = S$ and $\tau_1 = \frac{\sin(\beta)S^3(1-\alpha)|k_0|}{2\cos^2(\beta)}$, and convert the system of integral equations (3.11) into a scalar recurrence equation for the unknown real-valued coefficients τ_n. The Stokes constant, denoted finally by $K(\alpha;\beta)$, is now given by

$$K(\alpha;\beta) \equiv i\Gamma = 2\pi|k_0|\lim_{n\to\infty}\tau_n. \tag{4.4}$$

We note that this formula is valid for $\beta < \frac{\pi}{2}$, when the pole singularity occurs in the component $W(p)$ in (3.9). If $\beta > \frac{\pi}{2}$, the pole singularity occurs in the component $V(p)$, as per previous discussion. However, because of the relation $W(p) = V(-p)$, the same substitution (4.3) can be used with a modified definition of the Stokes constant $K(\alpha;\beta) = 2\pi|k_0|\lim_{n\to\infty}(-1)^n\tau_n = 2\pi|k_0|\lim_{n\to\infty}|\tau_n|$.

At each value of n, the recurrence equation for τ_n in terms of the coefficients $(\tau_0, ..., \tau_{n-1})$ is a linear equation of the form

$$\cos(\beta)\left(\frac{1}{2} - \frac{(2+(-1)^n)}{(n+2)(n+1)}\right)\tau_n = Q(\tau_0, \tau_1....\tau_{n-1}). \tag{4.5}$$

It is clear that equation (4.5) is non-singular for all $n \ge 1$ provided that $\cos(\beta) \ne 0$ (that is $\beta \ne \frac{\pi}{2}$). At $\beta = \pi/2$, $k_0 = 0$ and radiation modes are not exponentially small as $\kappa \to 0$ as shown in [17]. We shall consider the Stokes constant only for $\beta \in \left(\beta_0, \frac{\pi}{2}\right) \cup \left(\frac{\pi}{2}, \beta_1\right)$, since for $\beta < \beta_0$ and $\beta > \beta_1$, the pair $p = \pm ik_0$ does not give all roots of the dispersion relation on the imaginary axis. As a result, finding a simple zero of $K(\alpha;\beta)$ in these intervals is not sufficient for predicting bifurcations of a truly localised solution as we would also have to compute the Stokes constants for other modes corresponding to other eigenvalues on the imaginary axis.

In the case of the AL lattice ($\alpha = 1$), there exists an explicit travelling wave solution for all values of β and as mentioned in Section 2 this solution is captured by the first term of the asymptotic expansion, $\Phi_0(Z) = \mathrm{sech}(Z)$. Therefore we would expect that $K(1;\beta) \equiv 0$ for all β. Setting $\alpha = 1$ gives $\tau_0 = S = 1$ and $\tau_1 = 0$. If we assume that $\tau_1 = \tau_2 = ... = \tau_{n-1} = 0$ then a direct computation shows that τ_n is given by

$$\cos(\beta)\left(\frac{1}{2} - \frac{(2+(-1)^n)}{(n+2)(n+1)}\right)\tau_n = \begin{cases} \frac{(i|k_0|)^n}{(n+2)!}\tau_0\cos(\beta)(1-\tau_0^2) & \text{if } n \text{ is even,} \\ \frac{-|k_0|(i|k_0|)^{n-1}}{(n+2)!}\tau_0\sin(\beta)(1-\tau_0^2) & \text{if } n \text{ is odd.} \end{cases} \tag{4.6}$$

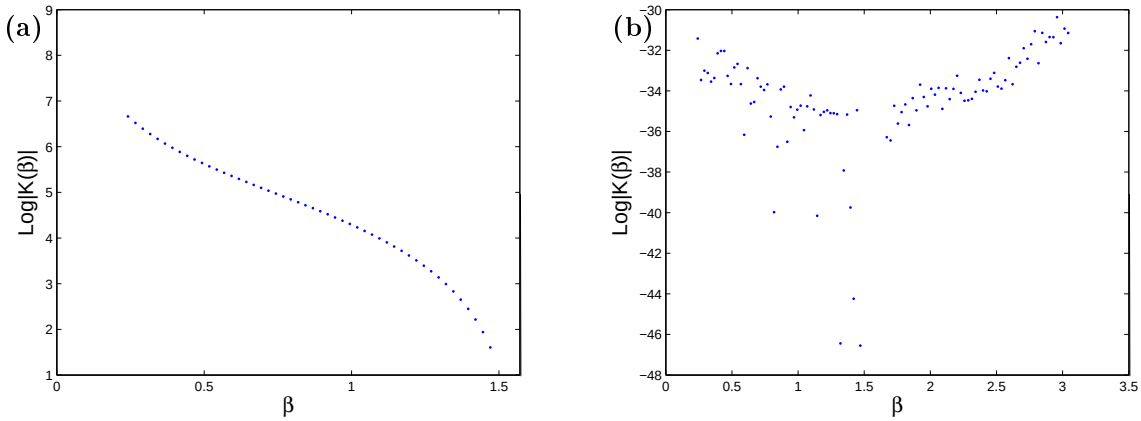

FIG. 4.1. *Computation of the Stokes constant $K(\alpha;\beta)$ for (a) cubic DNLS, $\alpha = 0$, and (b) AL model, $\alpha = 1$. There are no zeros of the Stokes constant for the cubic DNLS whilst the Stokes constant for the AL model is always zero (to numerical round off).*

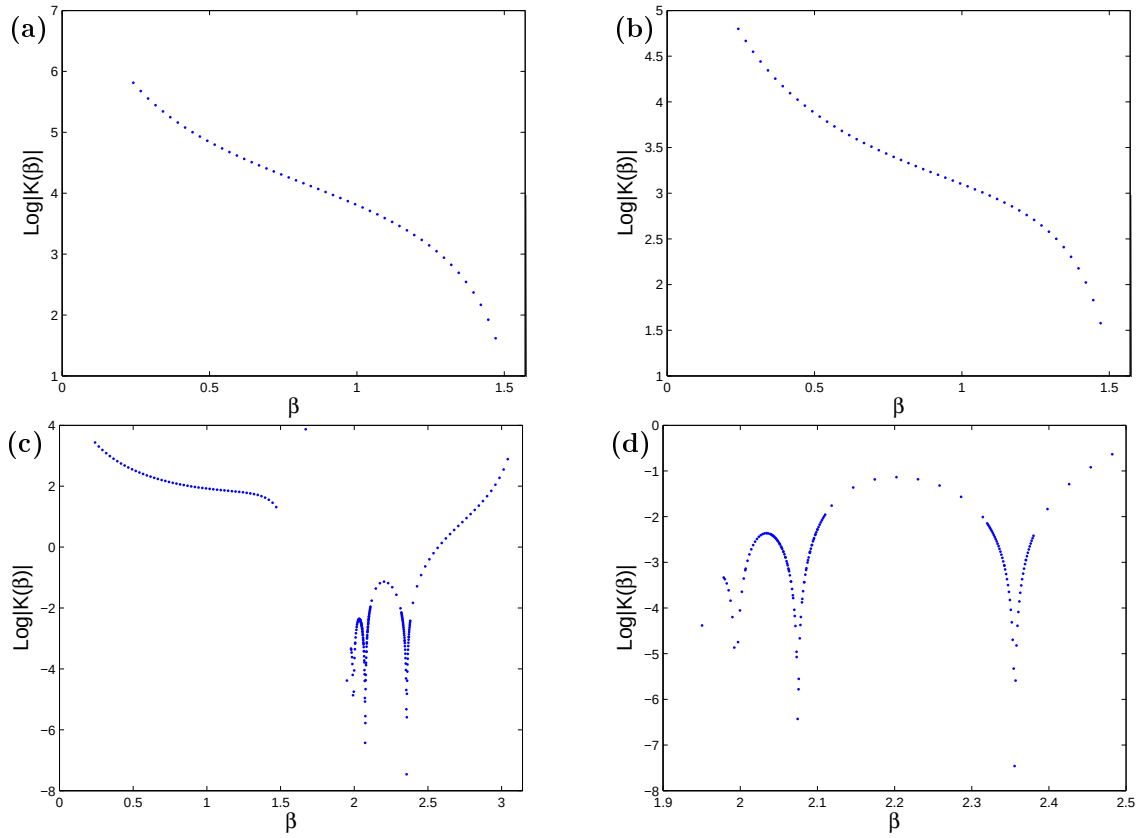

FIG. 4.2. *Computation of the Stokes constant $K(\alpha;\beta)$ for the Salerno model with varying β for $\alpha = 0.25$ (a), $\alpha = 0.5$ (b), and $\alpha = 0.75$ (c). The zoomed graph (d) shows that zeros of $K(\alpha;\beta)$ exist at $\beta \approx 1.98, 2.08, 2.36$ for $\alpha = 0.75$.*

Since for $\alpha = 1$, $\tau_0 = 1$ then the right hand side of (4.6) is equal to 0 and so $\tau_n = 0$ if $\tau_1 = ... = \tau_{n-1} = 0$. Therefore, indeed $K(1;\beta) \equiv 0$ for all values of β.

Equation (4.5) is computed numerically for a large value of n for fixed values of parameters (α, β) giving a good approximation to the Stokes constant. We are interested in the behaviour of $K(\alpha;\beta)$ as α and β are varied. First, let us consider the two limiting cases: the cubic DNLS model with $\alpha = 0$, where we expect the Stokes constant to be non-zero for all β, and the integrable AL model with $\alpha = 1$, where we have shown that $\tau_n = 0$ for all $n \geq 1$. These two models will give us a good check on the validity of the numerical code and are shown in Figure 4.1. The results

agree with our predictions. Indeed results of [14, 17] show that no single-humped localised travelling waves exist in the cubic discrete NLS model, while a two-parameter family of travelling wave solutions is known for the AL model.

Now we consider the intermediate values $\alpha \in (0,1)$. If $\alpha < 0.5$ then Figure 2.2 suggests that the computations must be restricted to the domain $\beta \in (\beta_0, \pi/2)$, where $\Phi_0 \in \mathbb{R}$. Figures 4.2 (a)-(b) show that no zeros of $K(\beta)$ are found for $\alpha \in [0, 0.5]$. If $\alpha > 0.5$, computations are extended to the domain $\beta \in (\beta_0, \pi/2) \cup (\beta_*, \beta_1)$. A number of zeros of $K(\beta)$ is found in the second interval (β_*, β_1), as is shown on Figures 4.2 (c)-(d). The number of zeros of $K(\alpha;\beta)$ depends on the value of α and each zero moves towards the point $\beta = \pi/2$ as $\alpha \to 1$. The existence of at least one travelling wave solution for $\beta > \pi/2$ agrees with the preliminary results in [16] where a travelling wave was found numerically for $\alpha = 0.7$ and $\beta = 0.875\pi$.

5. Numerical computation of travelling waves. The existence of a zero of the Stokes constant $K(\alpha;\beta)$ predicts a possible bifurcation of a travelling soliton, so we confirm here this prediction by finding localised solutions to the differential advance-delay equation (2.4). In addition, we test stability of localized solutions by direct numerical integration of the DNLS equation (1.1).

5.1. Localized solutions of the differential advanced-delay equation. To find localised solutions to the differential advance-delay equation (2.4) and to continue them as parameters vary, we use the method we have developed in earlier papers [12, 13, 16] based upon the earlier work of [2, 5, 6]. Specifically, a pseudo-spectral method is used to compute a numerical solution by extending $\Phi(Z)$ into a periodic function over a large finite domain $(-L/2, L/2)$,

$$\Phi(Z_i) = \sum_{j=1}^{N} a_j \cos\left(\frac{2\pi j}{L} Z_i\right) + i b_j \sin\left(\frac{2\pi j}{L} Z_i\right). \tag{5.1}$$

The differential advance-delay equation (2.4) is then decomposed into a large system of $2N+2$ algebraic equations posed on the collocation points $Z_i = \frac{Li}{2(N+1)}$ for $-(N+1) \le i \le (N+1)$ with the periodic boundary conditions $\Phi(Z_{N+1}) = \Phi(Z_{-(N+1)})$. This system is solved by using a Powell-hybrid method [18] and a localised solution, if it exists, is continued numerically in parameter space using AUTO [4]. By using an appropriate signed measure of the radiation tail amplitude, $\Delta = \mathrm{Im}(\Phi(L/2))$, based upon the symmetry of the periodic function, travelling localised solutions can be found as regular zeros of Δ, see [13]. Figures 5.1 (a,b) show the correspondence between zeros of the Stokes constant $K(\alpha;\beta)$, where there are four distinct zeros for $\kappa = 0$, and zeros of Δ, where there are two zeros for $\kappa = 0.5$, in the case $\alpha = 0.65$. The discrepancy in the number of zeros between the Stokes constant calculations and the pseudo-spectral computations is due to the fact that some of zeros of $K(\alpha;\beta)$ move to the domain $\beta > \beta_1 \approx \frac{13\pi}{14}$ for non-zero values of κ and hence do not generate bifurcations of non-trivial zeros of Δ.

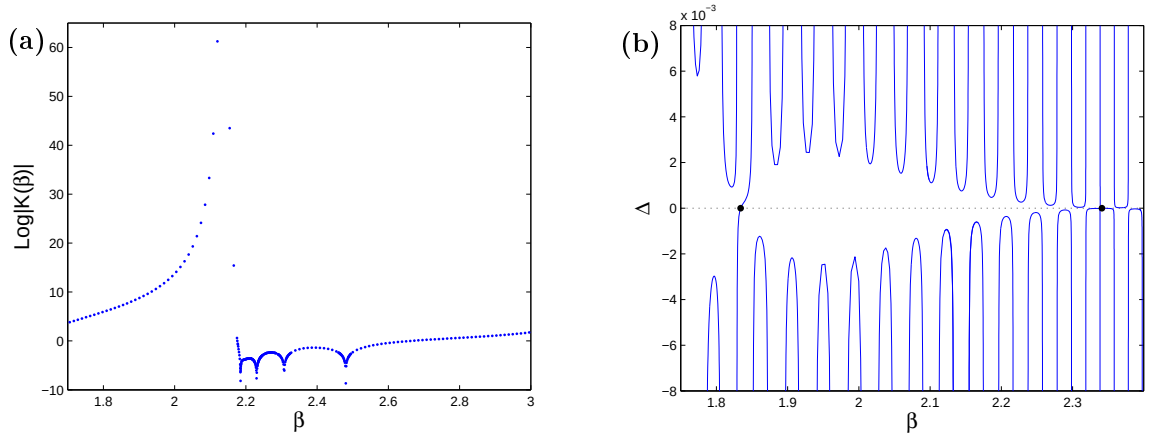

FIG. 5.1. *Existence of travelling wave solutions in the Salerno model for* $\alpha = 0.65$ *computed via calculation of (a) the Stokes constant* $K(\alpha;\beta)$ *(*$\kappa = 0$*) and (b) the radiation tail amplitude* Δ *(*$\kappa = 0.5$*). A number of points where localised waves exist are found, at* $\beta \approx 2.182, 2.237, 2.308$ *and* 2.48 *using the Stokes constant method and at* $\beta \approx 1.834, 2.34$ *from measuring the radiation tail amplitude (indicated by dots).*

We would expect the zeros of Δ to approach the zeros of $K(\alpha;\beta)$ as κ is reduced towards zero. However, since κ is a measure of the amplitude and width of the localised solution, continuing the solutions of the differential advance-delay equation (2.4) for small κ is a problematic computation as the solution becomes broad and has a small amplitude

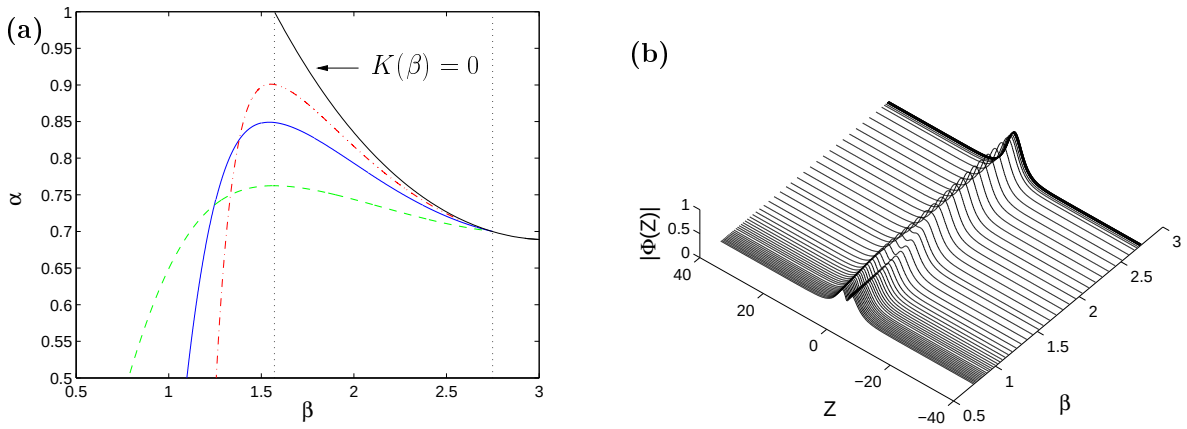

FIG. 5.2. *(a) Continuation of numerical solutions to the differential advance-delay equation (2.4) for varying α and β with $\kappa = 0.3$ (dash-dot line), $\kappa = 0.5$ (solid line) and $\kappa = 1$ (dashed line). As β is reduced, a fold bifurcation occurs and the single-humped solution splits into a double-humped one. Continuation of the first (i.e highest β) zero of the Stokes constant $K(\alpha;\beta)$ is shown as a solid black line. Dotted vertical lines indicate the special points $\beta = \pi/2$ and $\beta = \beta_1$. (b) Profiles $|\Phi(Z)|$ along the continuation branch with $\kappa = 0.5$ showing the splitting of single-humped solutions into double-humped ones.*

in this limit. It is a much easier task to compute continuation curves for a fixed non-zero value of κ in the (α, β)-plane and reduce the value of κ. Such continuations for non-zero κ are shown in Figure 5.2 (a). Also plotted in that figure is the line corresponding to the first (highest β) zero of $K(\alpha;\beta)$ which can be seen to approach the point $(\alpha, \beta) = (1, \frac{\pi}{2})$. Three curves of $\Delta = 0$ for $\kappa = 0.3, 0.5, 1$ are also shown. These curves approach the line $K(\alpha;\beta) = 0$ for $\beta > \frac{\pi}{2}$ as κ becomes smaller. All existence curves have a fold point at the maximum value of α for some value of $\beta < \pi/2$, which approaches the point $(\alpha, \beta) = \left(1, \frac{\pi}{2}\right)$ as $\kappa \to 0$. For β less than this fold point the solutions split into double-humped solutions as shown in panel (b).

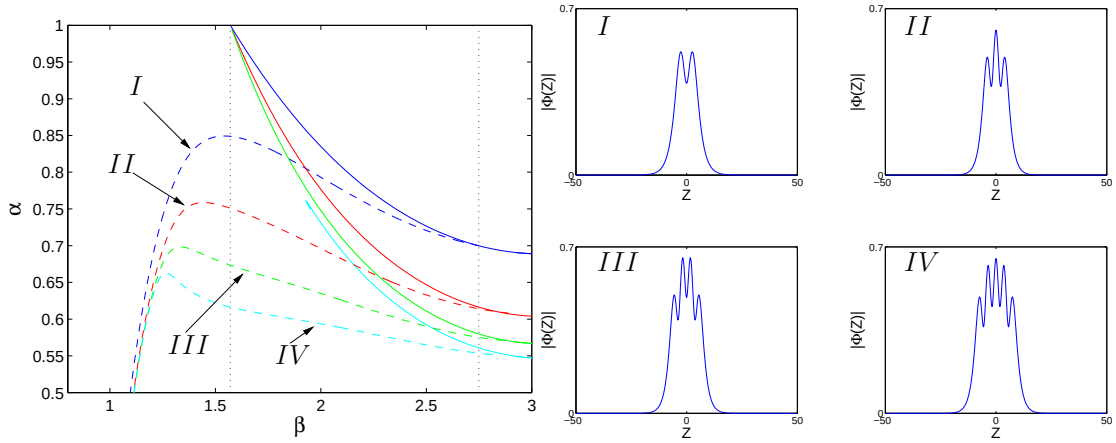

FIG. 5.3. *Continuation of zeros of the Stokes constants (solid lines) along with the corresponding branches of solutions with zero radiation tail $\Delta = 0$ for $\kappa = 0.5$ (dashed lines). For $\beta < \pi/2$ the solutions are multi-humped. The number of humps corresponding to each branch $(I - IV)$ is shown in the right panel, with $\alpha = 0.5$ for all plots and $\beta =$, I* 1.3267717242, *II* 1.2057587752, *III* 1.2167118387 *and IV* 1.1752123732.

Figure 5.3 illustrates the correspondence between subsequent zeros of $K(\alpha;\beta)$ shown by solid lines and zeros of Δ shown by dashed lines, for $\kappa = 0.5$. As in the previous case, all the lines of $K(\alpha;\beta) = 0$ seem to originate from the point $(\alpha, \beta) = (1, \frac{\pi}{2})$ and the numerical approximations to solutions obtained using the pseudo-spectral method match up well with the lines of $K(\alpha;\beta) = 0$ for $\beta > \frac{\pi}{2}$. In contrast, for $\beta < \frac{\pi}{2}$ the branches experience a fold with respect to α and the corresponding single-humped solutions become multi-humped solutions as β is decreased. The number of humps on each branch is shown in Figure 5.3, right panel. The number of humps increases as α is decreased for a fixed value of β. We emphasize that all curves of $K(\alpha;\beta) = 0$ on the figure are located in the domain where Φ_0 is real-valued.

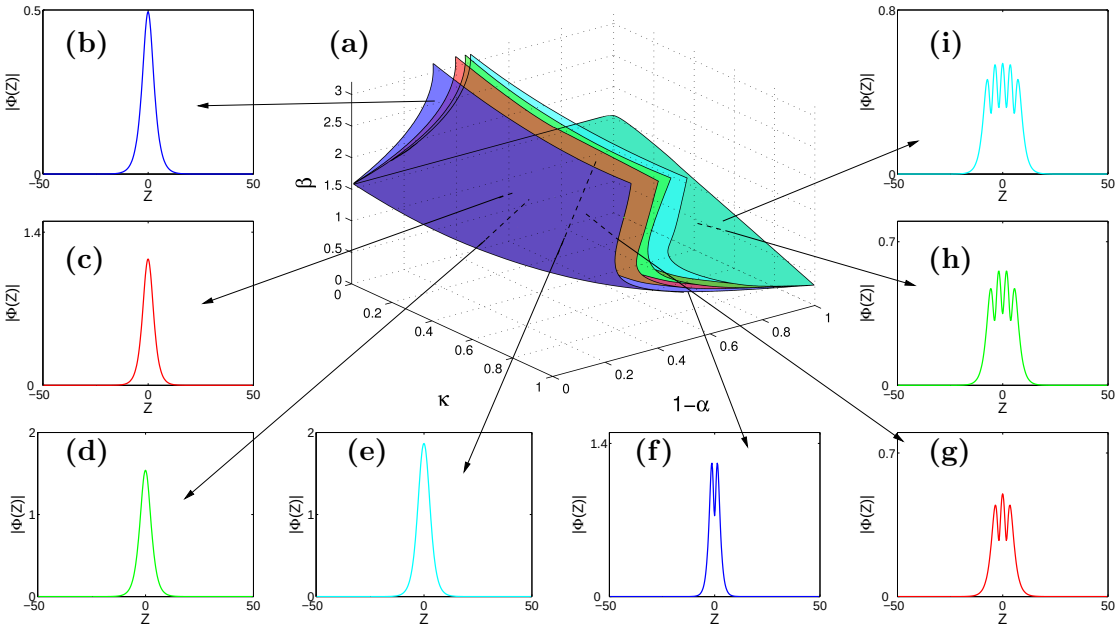

FIG. 5.4. *(a) Existence sketch of the first four "sheets" of solutions in $(\kappa, 1-\alpha, \beta)$-parameter space. (b)-(i) Profiles of solutions from different sheets showing single-humped solutions (b)-(e) for the upper surfaces and multi-hump solutions (f)-(i) on the lower surface. Colours on plots (b)-(i) match the solution sheet they originate from as shown in Figure 5.3.*

Figures 5.2 and 5.3 serve as illustration to two analytical results from [16, 17]. First, the branches of single-humped solutions for $\beta > \frac{\pi}{2}$ terminate for values of $\alpha > 0.5$ away from the cubic DNLS limit $\alpha \to 0$, while the branches of multi-humped solutions for $\beta < \frac{\pi}{2}$ extends to the cubic DNLS limit. Indeed, analysis of center manifold reductions near the point $\beta = \frac{\pi}{2}$ for the cubic DNLS model $\alpha = 0$ in [17] predicted an infinite number of branches of double-humped solutions and no single-humped solutions. On the other hand, both figures suggest that all solution branches for fixed values of κ have a fold point for $\alpha < 1$ away from the integrable AL limit $\alpha \to 1$. Indeed, by examining an appropriate Melnikov integral near the point $\beta = \frac{\pi}{2}$ it was found in [16] that the AL solutions do not persist for $\alpha \neq 1$ with a fixed value of $\kappa > 0$.

Figure 5.4(a) is a sketch of the four solution "sheets" in $(\kappa, 1-\alpha, \beta)$-space with solutions from each sheet in panels (b)-(i). When $\kappa = 0$, only the single-humped solutions for $\beta > \frac{\pi}{2}$ and $\alpha > 0.5$ exist, corresponding to the upper parts of the sheets, but as soon as κ is non-zero, an extra branch of multi-humped solutions for $\beta < \frac{\pi}{2}$ form, corresponding to the lower parts of the sheets. The fold point joining these two branches moves in the negative direction along the (α, β)-plane, such that the only time the sheet of solutions approaches the point of the integrable AL model ($\alpha = 1$) is at $\kappa = 0$, $\beta = \frac{\pi}{2}$. Behind the sheet of solutions shown, in the negative α direction, a number of other solution sheets exist and they correspond to the other solutions not shown in Figure 5.3. These solutions would be separate from all other sheets except at the point $(\alpha, \beta, \kappa) = (1, \frac{\pi}{2}, 0)$, although the multi-humped sheets become close to each other for $1 - \alpha$ sufficiently large and appear to merge on the line $\beta = \frac{\pi}{2}$ as $\kappa \to 0$.

5.2. Numerical integration of the DNLS equation. To simulate the single- and multi-humped solutions found previously in the initial-value problem associated with the DNLS equation (1.1), we use $h = 1$ and $u_n(t = 0) = \kappa\Phi(\kappa n)e^{i\beta n}$. Figure 5.5 shows the simulation of the single- and double-humped solutions for $\kappa = 0.5$ and $\alpha = 0.8$ across a lattice of N=800 sites centered initially on site n=400, where in all plots coloured areas signify non-zero amplitudes. It can be seen that the solitary waves remain localised throughout the duration of the simulation.

The stability of the solitary waves can be investigated by introducing a perturbation to the initial profile of the form $\mu u_n(0)$ where $u_n(0)$ is the unperturbed initial profile and $\mu \neq 1$. Figure 5.6 shows the motion of a perturbed single-humped solution from branch III with $\mu = 0.9$, panel (a), and a perturbed double-humped solution from branch I with $\mu = 1.1$, panel (b). After an initial (potentially long) transient period, where excess radiation is shed off, a perturbed single-humped solution carries on moving through the lattice without any more appreciable radiative losses (at least for a finite amount of time) see panel (a). In contrast, a perturbed multi-humped solution continuously emits radiation across the lattice until it is no longer localised, panel (b). Although only one example of the evolution of

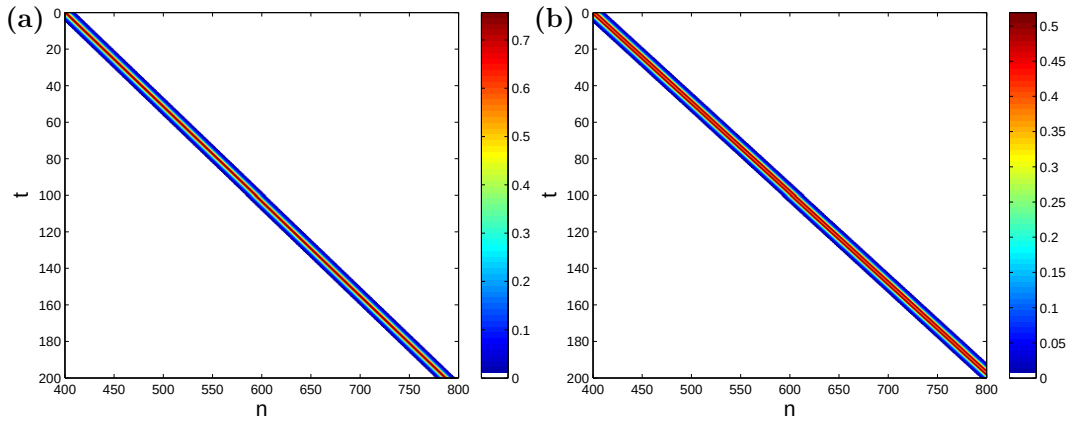

FIG. 5.5. *Direct integration of (a) single-humped and (b) double-humped solutions to the Salerno model for* $\alpha = 0.8$, $\kappa = 0.5$ *and (a)* $\beta = 1.9591683245$, *(b)* $\beta = 1.3267717242$. *Coloured regions indicate amplitudes significantly different from zero.*

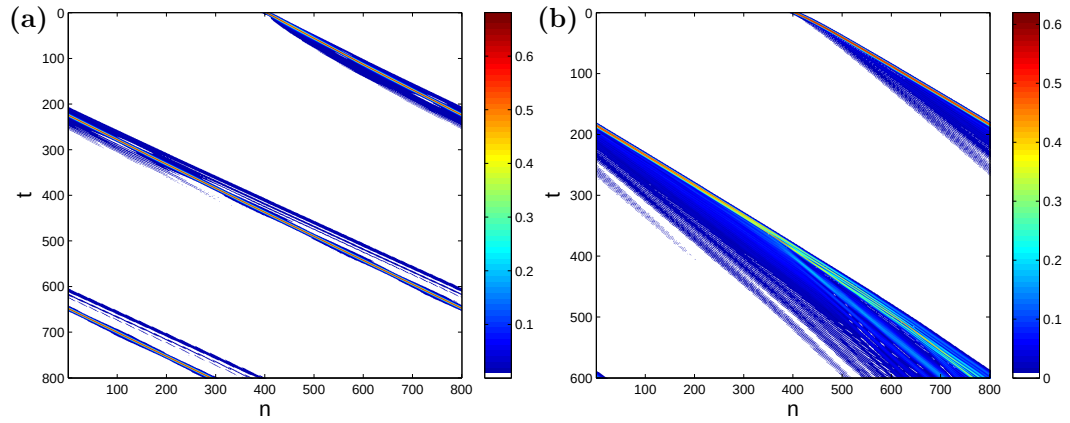

FIG. 5.6. *Perturbed solutions from branch I, (a) single-humped solution with* $\alpha = 0.65$, $\kappa = 0.5$, $\beta = 1.9591683245$ *and* $\mu = 0.9$, *(b) multi-humped solution with* $\alpha = 0.8$, $\kappa = 0.5$, $\beta = 1.3267717242$ *and* $\mu = 1.1$. *Qualitatively similar results are seen for single-humped and multi-humped solutions from all other branches.*

perturbed single- and multi-humped solutions is shown in Figure 5.6, we note that qualitatively similar results are observed for all other branches, with the single-humped solutions appearing stable and the multi-humped solutions unstable.

Collisions between two solutions for the same α values are shown in Figure 5.7 for a symmetric collision, between a single-humped solution and its reflected image. The collision is seen to be highly elastic with the motion of the solitons almost unaffected by the collision, although there is a slight variation in the amplitude of the solitons after collision. An asymmetric collision between a single-humped solution and a reflected multi-humped solution is shown in Figure 5.8. Here the effect of the collision is much greater with the multi-humped solution (travelling in the negative n direction) exhibiting a slowly decaying amplitude (panel (b)) whilst the single-humped solution exhibits a rapidly varying amplitude.

6. Conclusion. We have analysed the existence of localised travelling waves (homoclinic orbits to the rest state) in the Salerno model by computing zeros of the Stokes constant and homoclinic orbits of the differential advanced-delay equation. Branches of zeros of the Stokes constant were found to converge to the point $(\alpha, \beta) = (1, \frac{\pi}{2})$, which corresponds to the integrable AL lattice. Branches of travelling waves solutions were found along continuous curves in the (α, β)-plane. All solution families with non-zero values of κ were found not to intersect with the family of traveling wave solutions of the AL lattice. This result agrees with the Melnikov integral analysis [16] which states that the family of AL solutions at $\beta = \frac{\pi}{2}$ does not persist away from the limit $\alpha = 1$ for any finite value of κ.

We have also shown that existence curves for solutions of the differential advance-delay equation approach curves for zeros of the Stokes constant as κ gets smaller. To our knowledge, this is the first time that the relationship between

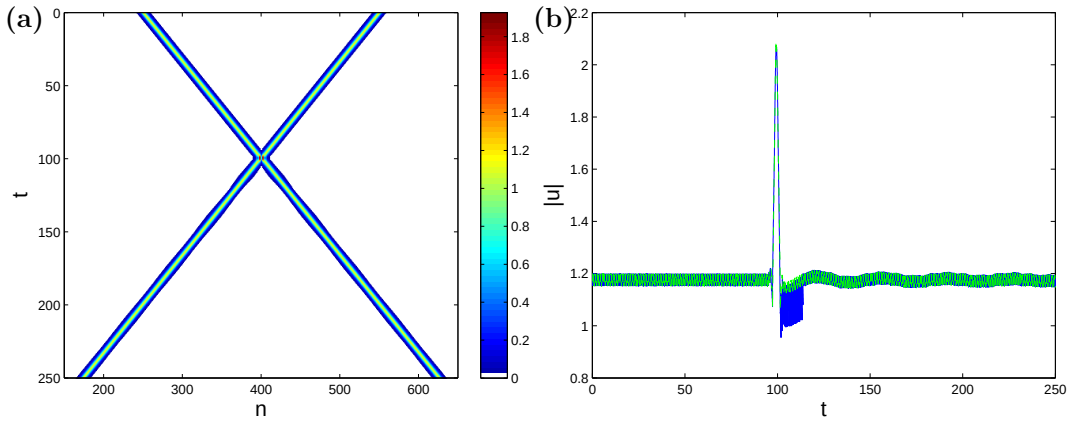

FIG. 5.7. *(a) Collision between a single-humped solution from branch II and its reflected image for $\alpha = 0.65$ and $\kappa = 0.5$ across a lattice for 250 time steps. (b) Amplitudes of each travelling wave as a function of time. The collision between the travelling waves appears to be nearly elastic.*

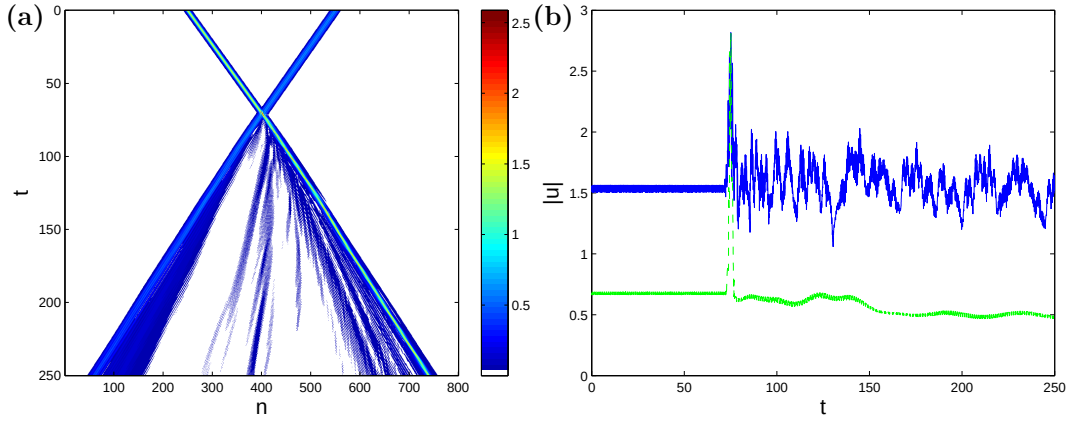

FIG. 5.8. *(a) Collision between a single-humped and a reflected multi-humped solution from branch III for $\alpha = 0.65$ and $\kappa = 0.5$ across a lattice for 250 time steps. (b) Amplitude of each travelling wave as a function of time. The single-humped solution is shown by solid blue line, while the multi-humped solution is shown by dashed green line.*

computation of Stokes constants and numerical solutions using a pseudo-spectral method has been illustrated; in particular this gives us valuable insight into the topology of the solution space. Branches of multi-humped solutions are also found for $\kappa \neq 0$, which are not predicted through analysis of the Stokes constants alone. The family of multi-humped solitons join the branch of single-humped solutions at a fold point that approaches the value $\beta = \frac{\pi}{2}$ as $\kappa \to 0$. The topology of the travelling waves in κ, β, α is interesting; there exists a number of solution 'sheets' nested one behind another that contain both single- and double-humped solutions joined by a fold for some value of $\beta \leq \frac{\pi}{2}$. The single-humped solutions only exist for $\alpha > 0.5$, at least for finite κ, and are therefore separated from the cubic DNLS limit $\alpha = 0$. The multi-humped solutions extend to the cubic DNLS limit. The solution sheets intersect the family of AL solutions only at the point $(\kappa, \beta, \alpha) = (0, \frac{\pi}{2}, 1)$ and are distinctly separate from the AL solutions at all other points.

Although we have shown the existence of travelling solutions in the Salerno model, there still remains the question of a full analysis of the stability and interactions of solutions. Our preliminary numerical computations show stability of single-humped traveling waves which have near-elastic collisions whilst multi-humped waves appear unstable. The question of whether there are an infinite or finite number of solutions sheets is also of interest. So far we have found four branches of solutions but it is highly likely that, in common with the DNLS with saturable nonlinearity [13], branches of solutions would become closer together and be numerically indistinct from each other as some limit is approached in the (α, β)-plane.

Acknowledgement. The authors would like to thank Robert McKay (Warwick) for useful conversations. This work was supported by the UK EPSRC.

REFERENCES

[1] M.J. Ablowitz and J.F. Ladik, "Nonlinear differential-difference equations and Fourier analysis", J. Math. Phys. **17**, 1011-1018 (1976)
[2] A.A. Aigner, A.R. Champneys and V.M Rothos, "A new barrier to the existence of moving kinks in Frenkel-Kontorova lattices", Physica D **186**, 148-170 (2003).
[3] D.N. Christodoulides, F. Lederer and Y. Silderberg, "Discretizing light behaviour in linear and nonlinear waveguide lattices", Nature **424**, 817-823 (2003)
[4] E.J. Doedel, *et al.* "Auto97 continuation and bifurcation software for ordinary differential equations", *ftp://ftp.es.concordia.ca/directory/doedel/auto* (1997)
[5] D.B. Duncan, J.C. Eilbeck, H.Feddersen and J.A.D. Wattis, "Solitons on lattices", Physica D **68**, 1–11 (1993)
[6] J.C. Eilbeck and R. Flesch, "Calculation of families of solitary waves on discrete lattices" Phys. Lett. A **149**, 200–202 (1990)
[7] S. Flach and K. Kladko, "Moving discrete breathers?" Physica D **127**, 61–72 (1999)
[8] J.W. Fleischer, T. Carmon, M. Segev, N.K. Efremidis and D.N. Christodoulides, "Observation of discrete solitons in optically induced real time waveguide arrays", Phys. Rev. Lett. **90**, 023902 (2003)
[9] J. Gómez-Gardeñes, L.M. Floria, M. Peyrard and A.R. Bishop, "Nonintegrable Scroödinger discrete breathers", Chaos **14**, 1130-1147 (2004)
[10] J. Gómez-Gardeñes, B.A. Malomed, L.M. Floria, and A.R. Bishop, "Discrete solitons and vortices in the two-dimensional Salerno model with coupling nonlinearities", Phys. Rev. E **74**, 036607 (2006)
[11] P.G. Kevrekidis, K.O. Rasmussen, and A.R. Bishop, "The discrete nonlinear Schrödinger equation: a survey of recent results", Int. J. Mod. Phys. B **15**, 2833–2900 (2001)
[12] T.R.O. Melvin, A.R. Champneys. P.G. Kevrekidis and J. Cuevas, "Radiationless Travelling Waves in Saturable Nonlinear Schrödinger Lattices", Phys. Rev. Lett. **97**, 124101 (2006)
[13] T.R.O. Melvin, A.R. Champneys, P.G. Kevrekidis and J. Cuevas, "Travelling Solitary Waves in the Discrete Nonlinear Schrödinger equation with Saturable nonlinearity: Existence, Stability and Dynamics", Preprint, *http://hdl.handle.net/1983/940*
[14] O.F. Oxtoby and I.V. Barashenkov, "Moving solitons in the discrete nonlinear Schödinger equation", Phys. Rev. E **76** 036603 (2007)
[15] D. Pelinovsky, "Translationally invariant nonlinear Schrodinger lattices", Nonlinearity **19**, 2695-2716 (2006)
[16] D.E. Pelinovsky, T.R.O. Melvin and A.R. Champneys, "One-parameter localized traveling waves in nonlinear Schrödinger lattices", Physica D **236**, 22-43 (2007)
[17] D.E. Pelinovsky and V.M. Rothos, "Bifurcations of travelling breathers in the discrete NLS equations", Physica D **202**, 16-36 (2005)
[18] M.J.D. Powell, "A hybrid method for nonlinear algebraic equations", in *Numerical Methods for Nonlinear Algebraic Equations* (Gordon and Breach, New York, 1970)
[19] M. Salerno, "Quantum deformations of the discrete nonlinear Schrdinger equation", Phys. Rev. A **46**, 6856–6859 (1992)
[20] A. Tovbis, M. Tsuchiya and C. Jaffé, "Exponential asymptotic expansions and approximations of the unstable and stable manifolds of singularly perturbed systems with the Hénon map as an example", Chaos **8**, 665-681 (1998)